



Cite this: *Chem. Commun.*, 2025, 61, 12361

Received 15th May 2025,  
Accepted 7th July 2025

DOI: 10.1039/d5cc02762d

[rsc.li/chemcomm](http://rsc.li/chemcomm)

## Bambusuril as an effective astatide sequestrating agent by hydrogen bonding†

Clémence Maingueneau,<sup>a</sup> Julie Patisson,<sup>b</sup> Marine Lafosse,<sup>b</sup> Elise Cartier,<sup>b</sup> Jean-François Gestin,<sup>a</sup> Grégory Pieters,<sup>b</sup> Frédéric Taran,<sup>b</sup> Jean-Pierre Dognon,<sup>c</sup> François Guérard<sup>a</sup> and Marie-Pierre Heck<sup>b</sup>

Herein, we report a molecular cage allowing strong chelation of the  $^{211}\text{At}^-$  radioanion. Propargylated bambus[6]uril shows good affinity towards iodide and astatide radiohalides, affording promising inclusion complexes that are stable in phosphate buffered saline and human serum. Density functional theory calculations support the presence of C–H $\cdots$ At non-covalent cooperative interactions governing the formation of astatinated cage complexes. To our knowledge, this work is the first to report  $^{211}\text{At}$ -labeling using encapsulation via hydrogen bonds, which opens new perspectives in the design of  $^{211}\text{At}^-$ -based radiopharmaceuticals.

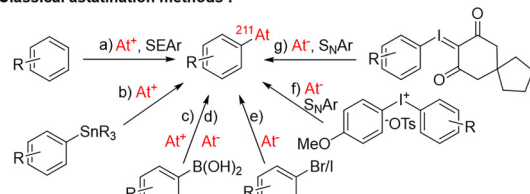
Radioisotopes of heavy halogens such as iodine I and astatine At are of significant interest in nuclear medicine for both imaging and therapeutic applications.<sup>1</sup> Astatine, the heaviest halogen of group 17 periodic elements, exists as 32 unstable isotopes. Among them,  $^{211}\text{At}$  is considered as one of the most promising  $\alpha$ -emitting radionuclides for targeted alpha therapy in cancer treatment.  $^{211}\text{At}$  exhibits several favorable properties for medical applications: a simple decay scheme leading in 100% of cases to the emission of one high energy (5.9–7.4 MeV), short track (50–90  $\mu\text{m}$ )  $\alpha$ -particle limiting irradiation of nearby healthy tissues, a short half-life (7.2 h) and a scalable production from a cheap  $^{209}\text{Bi}$ . Together, these features make  $^{211}\text{At}$  a radionuclide with high potential for effective targeted  $\alpha$ -therapies.<sup>2,3</sup> Consequently, several clinical trials of  $^{211}\text{At}$ -labeled drugs are currently underway.<sup>4</sup> Among its identified oxidation states (−1, 0, 1, 5, and 7), astatide  $\text{At}^-$  is the easiest species to obtain due to its stability in reducing media over a broad pH range.<sup>5</sup> As astatine has no stable isotope, iodine, its closest halogen neighbour with similar physico-chemical properties, is commonly used as a model of At. Therefore, iodine or general halogen chemistry is often applied to astatination although differences in chemical reactivity between the two elements

have also been reported.<sup>6</sup> Classical methods for  $\text{At}^-$  labelling generally afford aryl astatine–carbon bonds either by nucleophilic or electrophilic reactions (see Fig. 1(A)). Electrophilic substitutions occur with  $\text{At}^+$  species including direct aromatic electrophilic substitution (SEAr, Fig. 1(a)), astatodestannylation (Fig. 1(b)), and astatodeboronation (Fig. 1(c)), while nucleophilic substitutions with  $\text{At}^-$  species can be carried out through copper catalyzed astatodeboronation (Fig. 1(d)), halogen exchange (Fig. 1(e)), and  $\text{S}_{\text{N}}\text{Ar}$  reactions reported with arylidonium salts (Fig. 1(f)) or spirocyclic arylidonium ylides (Fig. 1(g)).<sup>7</sup>

Although several radiosynthesis routes can provide astatato-aryl compounds, their potential for *in vivo* applications is questioned by the low C–At bond stability predicted by theoretical calculations<sup>8</sup> and confirmed experimentally, leading to uncontrolled release of At in healthy organs.<sup>9</sup> To limit de-astatination, other bonding modalities have been studied such as B–At bonds in boron clusters;<sup>10</sup> metal–At bonds such as  $\text{AtHg}$ ,<sup>11</sup>  $\text{Rh}(\text{III})$  or  $\text{Ir}(\text{III})$ –(16anes<sub>4</sub>-diol)–At;<sup>12</sup> and  $\text{Rh}(\text{I})$ <sup>13</sup> or  $\text{Au}(\text{I})$ –NHC–At<sup>14</sup> complexes, which are, apart from metal toxicity, promising strategies for At-labeling.

In this context, using host molecules, promoting noncovalent interactions with the anion guest, can be an interesting approach to capture  $\text{At}^-$  through a host–guest complex

### A) Classical astatination methods :



### B) This work :

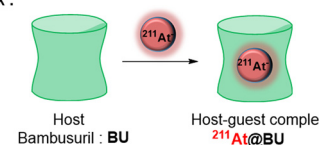


Fig. 1 (A) Classical methods for astatination, and (B) our approach.

<sup>a</sup> Nantes Université, Inserm, CNRS, Université d'Angers, CRCI2NA, Nantes, France.  
E-mail: [francois.guerard@univ-nantes.fr](mailto:francois.guerard@univ-nantes.fr)

<sup>b</sup> Université Paris-Saclay, CEA, INRAE, Département Médicaments et Technologie pour la Santé (DMTS), SCBM, 91191 Gif-sur-Yvette, France  
E-mail: [marie-pierre.heck@cea.fr](mailto:marie-pierre.heck@cea.fr)

<sup>c</sup> Université Paris-Saclay, CEA, CNRS, NIMBE, 91191 Gif-sur-Yvette, France

† Electronic supplementary information (ESI) available: Experimental section.  
See DOI: <https://doi.org/10.1039/d5cc02762d>



(Fig. 1(B), this work). Nevertheless, encapsulation of anions with a large atomic radius, low charge density and low ability to engage in hydrogen bonds is an important challenge.<sup>15</sup> In this regard, bambus[6]urils (**BU**s), synthetic neutral cavitands formed by six glycoluril units connected by six methylene bridges,<sup>16</sup> are known as the best large anion chelators, and their complexation properties for iodide, phosphate and perchlorate anions have been described.<sup>17</sup> Surprisingly, to the best of our knowledge, the use of **BU**s as radioactive anion-sequestering agents has not been reported so far. In this communication, we demonstrate the ability of  $R_{12}BU[6]$  ( $R = \text{propargyl}$ ) **BU 1** to act as a powerful  $^{125}\text{I}^-$  and  $^{211}\text{At}^-$  receptor by sequestering these radioactive anions, thanks to twelve cooperative hydrogen–radioanion interactions. While our experimental data highlight the (radio)stability of the obtained radioactive complexes, DFT calculations were employed to gain deeper insight into the interaction energies between the host (**BU**) and the two radioactive guests,  $^{125}\text{I}$  and  $^{211}\text{At}$ .

As we previously reported, **BU 1** (Scheme 1) exhibits high affinity for iodide, and crystals of  $\text{I}@\text{propargyl}_{12} \text{BU 2}$  confirmed the presence of the  $\text{I}^-$  anion within **BU**'s cavity.<sup>18</sup> Accordingly, **BU 1** was selected as a potential receptor for  $^{211}\text{At}^-$ . First, we investigated the binding properties of  $\text{Br}^-@\text{BU 1}$ <sup>19</sup> with  $\text{I}^-$  by  $^1\text{H}$  NMR titrations (see the ESI† for experimental procedures and data processing details). In  $\text{CD}_3\text{CN}$ , the stepwise addition of  $\text{I}^-$  to **BU 1** resulted in a slow exchange on the NMR timescale, indicating a strong affinity of **BU 1** for  $\text{I}^-$  ( $K_a = 4.4 \times 10^3 \text{ M}^{-1}$  in  $\text{CD}_3\text{CN}$ , see Fig. S1 and S2 in the ESI†). This result is consistent with the well-established higher affinity of bambusurils for  $\text{I}^-$  compared to  $\text{Br}^-$  anions.<sup>17,20</sup> The interaction between **BU 1** and  $\text{I}^-$  anions was also evaluated using isothermal titration calorimetry (ITC). In  $\text{MeOH}$ , **BU 1** exhibited a strong affinity for iodide ( $K_a = 2.1 \times 10^6 \text{ M}^{-1}$ , Fig. S3, ESI†). The ITC data clearly indicate that the formation of the  $\text{I}@\text{BU 2}$  complex is enthalpy-driven ( $\Delta H = -20.9 \text{ kJ mol}^{-1}$ ) and follows a 1:1 binding stoichiometry (Fig. S3, ESI†).<sup>20</sup> The measured affinity for iodide is comparable to values previously reported for bambusurils.<sup>17</sup>

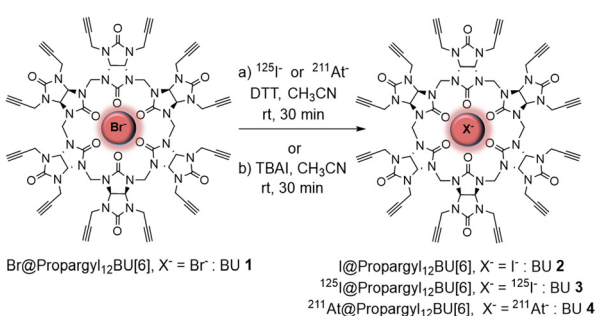
Based on these results, we investigated the complexation of  $^{211}\text{At}$  and  $^{125}\text{I}$  radioanions (used as a model of  $^{211}\text{At}$ ) with **BU 1** (Scheme 1). Preliminary experiments with sodium sulfite ( $\text{Na}_2\text{SO}_3$ ), sodium metabisulfite ( $\text{Na}_2\text{S}_2\text{O}_5$ ), and dithiothreitol

(DTT) were performed to identify a reductive agent capable of stabilizing  $^{211}\text{At}$  as the astatide species, amendable for the complexation reaction with **BU 1** in  $\text{CH}_3\text{CN}$  (see Table S1 and Fig. S4, ESI†). DTT appeared as the best reductive agent for astatine complexation with **BU 1**.

Although commercially available  $^{125}\text{I}$  is provided as sodium iodide in basic solution ( $\text{NaOH}$ ), DTT was added to the  $^{125}\text{I}[\text{NaI}]$  solution to study the complexation under the same experimental conditions as those used for  $^{211}\text{At}$ . The non-radioactive iodinated complex  $\text{I}@\text{propargyl}_{12}\text{BU 2}$ <sup>18</sup> was first prepared as an analytical reference of  $^{125}\text{I}@\text{BU 3}$  and  $^{211}\text{At}@\text{BU 4}$  radiocomplexes. **BU 2** was synthesized from  $\text{Br}^-@\text{BU 1}$  and TBAI (tetrabutylammonium iodide) in  $\text{CH}_3\text{CN}$  (90% yield), as reported in Scheme 1, conditions (b). Then, radiolabelled complexes  $^{125}\text{I}@\text{BU 3}$  and  $^{211}\text{At}@\text{BU 4}$  were prepared from **BU 1** (1.2 mM in  $\text{CH}_3\text{CN}$ ) by adding a solution of  $^{125}\text{I}$  or  $^{211}\text{At}$  in the presence of DTT (see ESI† and Fig. S5 for details). After 30 min at room temperature, the complexes  $^{125}\text{I}@\text{BU 3}$  and  $^{211}\text{At}@\text{BU 4}$  were obtained in very good radiochemical yields (RCYs), 99% and 90%, respectively. These results showed that the radiocomplexation reactions of  $^{125}\text{I}$  and  $^{211}\text{At}$  are rapid and that the radiolabelled complexes **BU 3–4** are stable and detectable at trace radionuclide concentrations, demonstrating the capacity of **BU 1** to efficiently encapsulate radioactive iodide and astatide anions. Complexes **BU 3–4** were identified by radio-HPLC analysis. As expected, nearly identical retention times were obtained for  $^{211}\text{At}@\text{BU 4}$ ,  $^{125}\text{I}@\text{BU 3}$  and non-radioactive iodinated reference  $\text{I}@\text{BU 2}$  (see Fig. S6, ESI†).

Subsequently, various **BU** concentrations and solvents were studied as they can influence radioanion complexation (see Fig. S7–S10, ESI†).  $^{125}\text{I}$  and  $^{211}\text{At}$  radioanions reacted at room temperature for 30 min with varying concentrations of **BU 1** in  $\text{CH}_3\text{CN}$ ,  $\text{CH}_2\text{Cl}_2$  or  $\text{CHCl}_3$  solutions (see Fig. 2(A) and (B)). Starting from **BU 1** (a concentration of 293.9  $\mu\text{M}$ ), the corresponding complexes  $^{211}\text{At}@\text{BU 4}$  (Fig. 2(A) and Fig. S7, ESI†) and  $^{125}\text{I}@\text{BU 3}$  (Fig. 2(B) and Fig. S8 and S9, ESI†) were obtained in high RCYs (90%, 88%, and 91%) for  $^{211}\text{At}@\text{BU 4}$  and (99%, 99%, and 99%) for  $^{125}\text{I}@\text{BU 3}$  in  $\text{CH}_3\text{CN}$ ,  $\text{CH}_2\text{Cl}_2$ , and  $\text{CHCl}_3$ , respectively. The efficient complexation of  $^{211}\text{At}@\text{BU 4}$  in  $\text{CHCl}_3$  is very promising as purified  $^{211}\text{At}$  is frequently delivered in  $\text{CHCl}_3$ . Given the limited radiolabelling reactions described in  $\text{CHCl}_3$ , complexation can be performed immediately after astatide purification, avoiding the additional concentration evaporation step usually required. We observed that  $^{125}\text{I}@\text{BU 3}$  and  $^{211}\text{At}@\text{BU 4}$  complexes are formed within 10 min of reaction, indicating rapid anion capture kinetics (Fig. S9 and S10, ESI†). The radiolabelled  $^{125}\text{I}@\text{BU 3}$  and  $^{211}\text{At}@\text{BU 4}$  complexes were subsequently purified on a silica cartridge before further evaluation (see the ESI† for details).

Then, the stabilities of radiocomplexes  $^{125}\text{I}@\text{BU 3}$  and  $^{211}\text{At}@\text{BU 4}$  were evaluated in human blood serum (HS) at 37 °C and phosphate buffered saline (PBS) at room temperature (see Fig. 2(C), (D) and Fig. S11–S14, ESI†). In fact, as bambusurils have a strong affinity for anions, PBS is an interesting medium to study as it contains chlorides, at the same concentration and same pH (7.4) as in the blood, which are potential competitors of  $\text{At}^-$ . Both  $^{125}\text{I}@\text{BU 3}$  and  $^{211}\text{At}@\text{BU 4}$  showed



Scheme 1 Synthesis of  $^{125}\text{I}@\text{BU 3}$  and  $^{211}\text{At}@\text{BU 4}$  radiocomplexes (conditions a) and  $\text{I}@\text{BU 2}$  (conditions b).



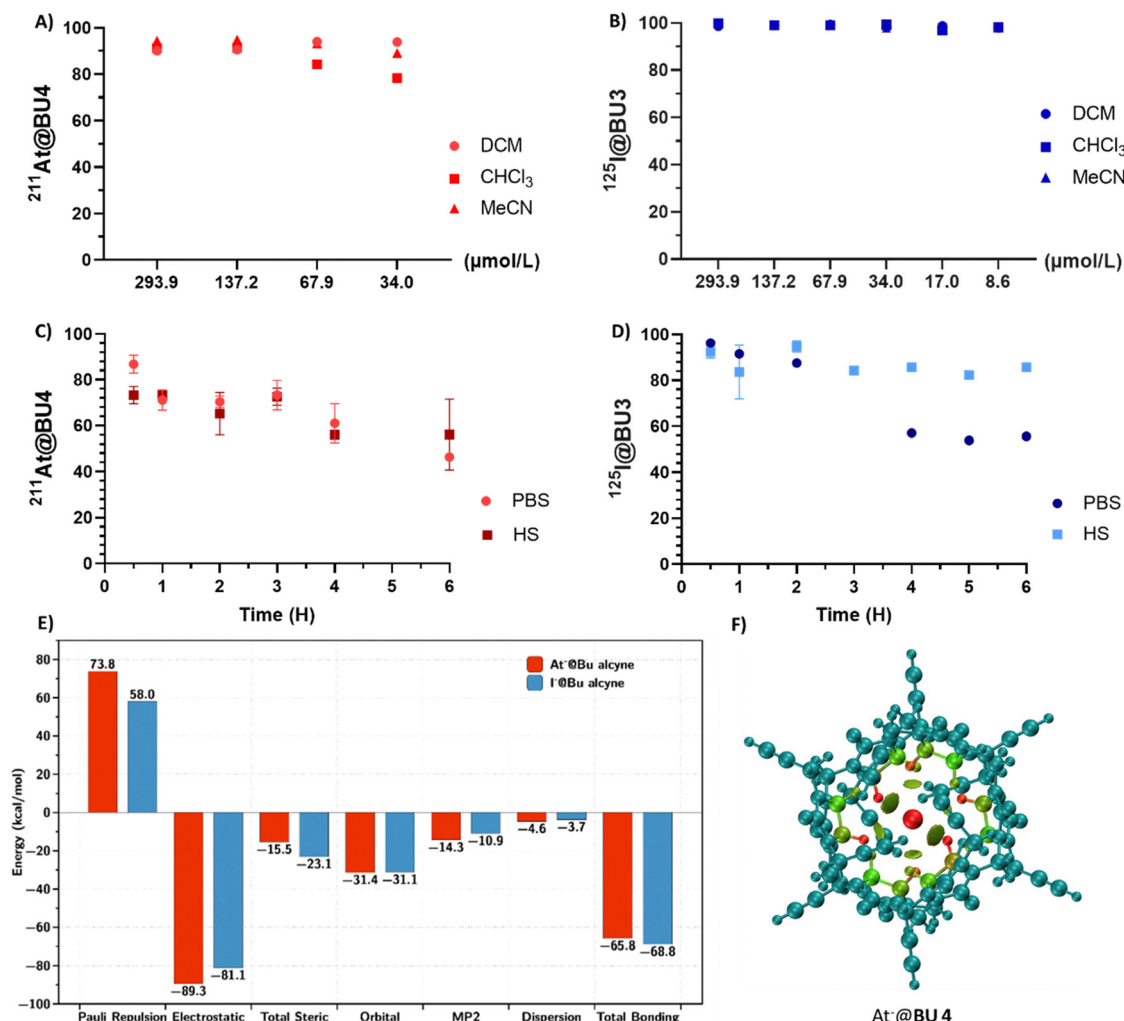


**Fig. 2** (A) Influence of the **BU 1** concentration on radiolabelling of  $^{211}\text{At}$  in DCM (●),  $\text{CHCl}_3$  (■), and  $\text{CH}_3\text{CN}$  (▲); (B) influence of the **BU 1** concentration on radiolabelling of  $^{125}\text{I}$  in DCM (●),  $\text{CHCl}_3$  (■), and  $\text{CH}_3\text{CN}$  (▲), standard conditions: 0.5–1.5 MBq, DTT (0.16  $\mu\text{mol}$ ), at rt for 30 min, with RCY determined by TLC; (C) stability study of  $^{211}\text{At}$ @**BU 4** in PBS (●) and in HS (■) at 37 °C; (D) stability study of  $^{125}\text{I}$ @**BU 3** in PBS (●) and in HS (■) at 37 °C with RCY (%) as a function of time (hours); (E) bonding energy analysis using ZORA-DFT with the revDOD-PBE-D4 functional, focusing on interactions between  $\text{At}^-/\text{I}^-$  and **BU 1** fragments (see the ESI† for details); (F) isosurface map to visualize  $\text{C}-\text{H}\cdots\text{At}$  non-covalent interactions in **BU 4**; for ease of reading, only H atom interactions with **At** are shown. The molecular structure is color-coded according to the contribution of various atoms to the interfragment interaction, using a blue-green-red color scale. Atoms appearing in red indicate a greater involvement in the **At-BU** cage interaction, highlighting regions of stronger interactions.

some dehalogenation in PBS but remained mostly intact after 6 h of incubation (60% and 55%, respectively, see Fig. 2(C), (D) and Fig. S11, S12, ESI†). In HS, the stability of the complexes was higher than in PBS, again with a slight superiority of  $^{125}\text{I}$ @**BU 3** over  $^{211}\text{At}$ @**BU 4** (80% and 70% of intact complex after 6 h, respectively, see Fig. 2(C) and (D) and Fig. S13 and S14, ESI†). Overall, observing the retention of  $^{125}\text{I}$  and  $^{211}\text{At}$  in the **BU**'s cage over several hours validates our complexation concept and the strong encapsulation of these halides.

To gain deeper insights into the stability of the  $^{125}\text{I}$ @**BU 3** and  $^{211}\text{At}$ @**BU 4** complexes, density functional theory (DFT) calculations were performed. The factors affecting the stability of the **BU 1** complexes with  $\text{I}^-$  and  $\text{At}^-$  anions were analyzed using an energy decomposition approach (see Fig. 2(E) and Fig. S15, ESI† for details). For both complexes  $^{211}\text{At}$ @**BU 4** and

$^{125}\text{I}$ @**BU 3**, similar trends were observed in the noncovalent interactions involved. The dominant contribution to the interaction energy arises from the electrostatic interaction, accounting for approximately 64% of the total attractive interactions in both complexes. This is followed by orbital interactions, contributing around 22.5% for  $^{211}\text{At}$ @**BU 4** and 24.5% for  $^{125}\text{I}$ @**BU 3**. To a lesser extent, the MP2 interaction energies associated with the noncovalent  $\text{C}-\text{H}\cdots\text{X}$  interaction are also notable, with values of approximately 10.9 kcal mol<sup>-1</sup> for  $^{211}\text{At}$ @**BU 4** compared to 8.6 kcal mol<sup>-1</sup> for  $^{125}\text{I}$ @**BU 3**. Finally, dispersion interactions further contribute to the overall stability of the complexes. The total bonding energy for  $\text{I}^-$  and  $\text{At}^-$  exhibits a difference of 3 kcal mol<sup>-1</sup>, with greater stabilization observed in the  $^{125}\text{I}$ @**BU 3** complex ( $-68.8$  versus  $-65.8$  kcal mol<sup>-1</sup> for I and At, respectively). This indicates that **BU 1** has a slightly higher

affinity for iodide than for astatide. This trend has been confirmed experimentally since the **BU 1** concentration can be decreased by 8-fold (34  $\mu\text{mol L}^{-1}$ ) for complexation with  $^{211}\text{At}$  and by 32-fold (8.6  $\mu\text{mol L}^{-1}$ ) for  $^{125}\text{I}$  @ **BU 3** formation, without affecting the RCY (see Fig. S7–S10, ESI $\dagger$ ). Here, the difference in the stability of the two complexes ( $^{211}\text{At}$  @ **BU 4** and  $^{125}\text{I}$  @ **BU 3**) could be explained by either this slightly lower affinity of  $\text{At}^-$  *versus*  $\text{I}^-$  or the tendency of  $\text{At}^-$  to be oxidized in the  $\text{At}^+$  cation exhibiting no affinity for the **BU 1** cage.<sup>5</sup>

Quantum chemical calculations were also employed to determine the volume of the central bambusuril cavity, for both the empty **BU** cage and the anions encapsulated (see Fig. S16 and S17, ESI $\dagger$ ). The volume of the central cavity in the empty **BU**'s cage **BU 1** was found to be 32.6 Å. In the presence of astatide and iodide anions, the cavity volume decreased to 32.0 Å and 31.5 Å, respectively. The smaller cavity size observed with iodide compared to astatine suggests a stronger interaction between the iodide anion and the cage, consistent with the interaction energy analysis. Furthermore, the non-covalent  $\text{C}-\text{H}\cdots\text{I}$  and  $\text{C}-\text{H}\cdots\text{At}$  interactions in  $\text{I}$  @ **BU 3** and  $\text{At}$  @ **BU 4** were analyzed using Multiwfn software<sup>21</sup> (Fig. 2(F) and Fig. S14, ESI $\dagger$ ). The computed isosurfaces (green regions) clearly highlight the presence of  $\text{C}-\text{H}\cdots\text{I}$  interactions (Fig. S16(a), ESI $\dagger$ ) and  $\text{C}-\text{H}\cdots\text{At}$  interactions (Fig. 2(F) and Fig. S16(b), ESI $\dagger$ ).

In summary, we report the first radiolabelling of a **BU**[6] cage with astatine-211 and iodine-125, yielding stable  $^{211}\text{At}$  @ **BU 4** and  $^{125}\text{I}$  @ **BU 3** complexes in both organic and biologically relevant media. These experimental and theoretical results constitute the first evidence of astatide sequestration within a host molecule through hydrogen bond interactions, demonstrated here using a bambusuril cage. To our knowledge, radiopharmaceuticals based on anion chelation remain unexplored, in contrast to the widespread use of cation-complexing agents with radiometals in nuclear medicine.<sup>22</sup> This preliminary study thus paves the way for new opportunities in the field of radiopharmaceuticals.

This work was financially supported by the “Ministère de l'Education nationale de l'Enseignement supérieur et de la Recherche”, the French National Agency for Research (ANR-24-CE07-5913 and ANR-11-LABX-18-01 (Labex IRON)), and the INCa-DGOS-INSERM-ITMO Cancer\_18011. The Radioactivity Technical Platform (SFR Santé François Bonamy) is thanked for the technical support, and the Arronax GIP is acknowledged for providing  $^{211}\text{At}$ . The “Service de Chimie Bioorganique et de Marquage” (SCBM, CEA) is a partner of NOMATEN, a Centre of Excellence in Multifunctional Materials for Industrial and Medical Applications (EU H2020 Teaming #857470).

## Conflicts of interest

There are no conflicts to declare.

## Data availability

The data supporting this article have been included as part of the ESI. $\dagger$

## Notes and references

- R. Eychenne, C. Alliot, J.-F. Gestin and F. Guérard, *Nuclear Medicine and Molecular Imaging*, Elsevier, Oxford, 2022, pp. 121–132.
- S. Lindegren, P. Albertsson, T. Bäck, H. Jensen, S. Palm and E. Aneheim, *Cancer Biother. Radiopharm.*, 2020, **35**, 425.
- (a) R. Eychenne, M. Chérel, F. Haddad, F. Guérard and J.-F. Gestin, *Pharmaceutics*, 2021, **13**, 906; (b) R. Zimmermann, *J. Nucl. Med.*, 2025, **66**, 681.
- P. Albertsson, T. Bäck, K. Bergmark, A. Hallqvist, M. Johansson, E. Aneheim, S. Lindegren, C. Timperanza, K. Smerud and S. Palm, *Front. Med.*, 2022, **9**, 1076210.
- (a) L. Liu, R. Maurice, N. Galland, P. Moisy, J. Champion and G. Montavon, *Inorg. Chem.*, 2022, **34**, 13462; (b) A. N. Espino-Vásquez, F. C. Rojas-Castro and L. Mitzuko Fajardo-Yamamoto, *Future Pharmacol.*, 2022, **4**, 377.
- F. Guérard, C. Maingueneau, L. Liu, R. Eychenne, J.-F. Gestin, G. Montavon and N. Galland, *Acc. Chem. Res.*, 2021, **54**, 3264.
- (a) M. Vanermen, M. Ligeour, M.-C. Oliveira, J.-F. Gestin, F. Elvas, L. Navarro and F. Guérard, *EJNMMI Radiopharmacy Chem.*, 2024, **9**, 69; (b) T. Dong, Z. Zhang, W. Li, W. Zhuo, T. Cui and Z. Li, *J. Org. Chem.*, 2024, **89**, 11837.
- M. Amaouch, G. Montavon, N. Galland and J. Pilme, *Mol. Phys.*, 2016, **114**, 1326.
- (a) D. S. Wilbur, *Curr. Radiopharm.*, 2008, **1**, 144; (b) D. Teze, D.-C. Sergentu, V. Kalichuk, J. Barbet, D. Deniaud, N. Galland, R. Maurice and G. Montavon, *Sci. Rep.*, 2017, **7**, 2579.
- D. S. Wilbur, M.-K. Chyan, D. K. Hamlin, R. L. Vessella, T. J. Wedge and M. F. Hawthorne, *Bioconjugate Chem.*, 2007, **18**, 1226.
- M. Pruszynski, A. Bilewicz, B. Was and B. Petelenz, *J. Radioanal. Nucl. Chem.*, 2006, **268**, 91.
- M. Pruszynski, A. Bilewicz and M. R. Zalutsky, *Bioconjugate Chem.*, 2008, **19**, 958.
- H. Rajerison, F. Guérard, M. Mougin-Degraef, M. Bourgeois, I. Da Silva, M. Chérel, J. Barbet, A. Faivre-Chauvet and J.-F. Gestin, *Nucl. Med. Biol.*, 2014, **41**, e23.
- M. Ligeour, S. G. Guillet, C. Maingueneau, M. Croyal, A. Planchat, J.-F. Gestin, N. Galland and F. Guérard, *Chem. – Eur. J.*, 2025, e202500826.
- (a) M. J. Langton, *Angew. Chem., Int. Ed.*, 2016, **55**, 1974; (b) F. Biedermann, W. M. Nau and H.-J. Schneider, *Angew. Chem., Int. Ed.*, 2014, **53**, 11158; (c) S. Kubik, *Chem. Soc. Rev.*, 2010, **39**, 3648; (d) Q.-X. Liu, J.-R. Chen, X.-F. Sun, X.-J. Zhao and K.-Q. Cai, *RSC Adv.*, 2016, **6**, 12256; (e) H.-J. Schneider, *Angew. Chem., Int. Ed.*, 2009, **48**, 3924.
- (a) J. Svec, M. Necas and V. Sindelar, *Angew. Chem., Int. Ed.*, 2010, **49**, 2378–2381; (b) T. Fiala, K. Slezáková, K. Marsalek, K. Salvadori and V. Sindelar, *J. Org. Chem.*, 2018, **83**, 1903; (c) J. Rivollier, P. Thuéry and M.-P. Heck, *Org. Lett.*, 2013, **15**, 480; (d) D. Azazna, M. Lafosse, J. Rivollier, J. Wang, I. Ben Cheikh, M. Meyer, P. Thuéry, J.-P. Dognon, G. Huber and M.-P. Heck, *Chem. – Eur. J.*, 2018, **24**, 10793; (e) M. Singh, E. Solel, E. Keinan and O. Reany, *Chem. – Eur. J.*, 2016, **22**, 8848; (f) P. Mondal, E. Solel, N. Fridman, E. Keinan and O. Reany, *Chem. – Eur. J.*, 2019, **25**, 13336.
- (a) V. Havel and V. Sindelar, *ChemPlusChem*, 2015, **80**, 1601; (b) T. Lízal and V. Sindelar, *Isr. J. Chem.*, 2018, **58**, 326; (c) M. Chvojka, D. Madea, H. Valkenier and V. Šindelář, *Angew. Chem., Int. Ed.*, 2024, **63**, e202318261; (d) M. Lafosse, Y. Liang, J. P. Schneider, E. Cartier, A. Bodlener, P. Compain and M.-P. Heck, *Molecules*, 2022, **27**, 4772.
- M. Lafosse, E. Cartier, K. Solmont, J. Rivollier, D. Azazna, P. Thuéry, Y. Boulard, A. Gontier, J.-B. Charbonnier, B. Kuhnast and M.-P. Heck, *Org. Lett.*, 2020, **22**, 3099.
- $\text{Br}^-$  @ **BU 1** was chosen due to its good solubility in  $\text{CH}_3\text{CN}$  compared to insoluble anion-free **BU 1**.
- (a) R. Ghai, R. J. Falconer and B. M. Collins, *J. Mol. Recognit.*, 2012, **25**, 32; (b) T. Wiseman, S. Williston, J.-F. Brandts and L. Lin, *Anal. Biochem.*, 1989, **179**, 131.
- T. Lu, *J. Chem. Phys.*, 2024, **161**, 082503.
- Q. Peña, A. Wang, O. Zaremba, Y. Shi, H. W. Scheeren, J. M. Metselaar, F. Kiessling, R. M. Pallares, S. Wuttke and T. Lammers, *Chem. Soc. Rev.*, 2022, **51**, 2544.

